

# Dynamic Hyperpolarized C-13 Spectroscopic Imaging using Radial Acquisition and HYPR Reconstruction

K. Wang<sup>1</sup>, E. Peterson<sup>2</sup>, J. Gordon<sup>1</sup>, K. Kurpad<sup>3</sup>, I. Rowland<sup>3</sup>, M. Erickson<sup>3</sup>, and S. Fain<sup>1</sup>

<sup>1</sup>Medical Physics, University of Wisconsin-Madison, Madison, WI, United States, <sup>2</sup>Biomedical Engineering, University of Wisconsin-Madison, Madison, WI, United States, <sup>3</sup>Radiology, University of Wisconsin-Madison, Madison, WI, United States

## INTRODUCTION

Hyperpolarized (HP) C-13 compounds exhibit non-equilibrium  $T_1$  decay and rapidly evolving spectral dynamics, and it is highly desirable to develop pulse sequences to image C-13 compounds in the spatial-spectral-time domain with high resolution in all dimensions. However, due to the dominance of  $T_1$  decay over recovery, every RF excitation consumes a fraction of the total magnetization, and therefore sets a limit on the total number of RF pulse that can be played out during the entire imaging protocol. This unique property makes non-Cartesian sampling methods such as radial acquisition (1) and spiral imaging (2) very attractive due to their reduced sensitivity to under-sampling artifacts. In this work, we propose a radial EPSI (3) acquisition method that is designed for HP C-13 time-resolved spectroscopic imaging. In particular, we used a HYPR (4) algorithm along the time dimension to further suppress streak artifacts and to improve SNR.

## THEORY

The proposed method, shown in Fig. 1, is summarized as follows. **Step 1:** For each time frame, a radial multi-echo acquisition sequence with fly-back gradient is used to acquire a few projections with spatial undersampling but fully-resolved spectrum. This acquisition is repeated for all the other time frames with interleaved projection angles. Here bit-reversal angle ordering is used for both inter and intra time frame view-ordering schemes to avoid dominant projections from similar directions. **Step 2:** After scanning, radial data for each individual frame are reconstructed by filtered back-projection (FBP) and Fourier transformed along the echo dimension, generating undersampled spectroscopic images at all time frames. **Step 3:** HYPR (4) can then be performed on selected spectral image of interest, e.g. lactate image. Specifically, undersampled lactate images from all time frames were averaged to form a composite image. Then a weighting image can be synthesized by normalizing an unfiltered back-projection time frame by a re-sampled composite image. Finally, the lactate HYPR image is calculated as the product of the composite image and the weighting image. The HYPR processing step can then be repeated for another selected species, e.g. pyruvate.

## MATERIALS AND METHODS

The proposed method was first validated using computer simulations in Matlab (The Mathworks, Inc., Natick, MA, USA). Two disks (big and small) were simulated in the numerical phantom. In order to account for signal changes due to  $T_1$  decay and metabolic processes; a set of in-vivo dynamic spectroscopy data was acquired, which included the effect of the first two factors. Simulation parameters included:  $64 \times 64$  matrix,  $FA=10^\circ$ , 8 time frames with only 16 projections per time frame. For each radial readout, 32 echoes with  $\Delta TE=1.3ms$  (spectral resolution of 24Hz) were simulated. The dynamic spectroscopy data were acquired on a Varian small animal 4.7T scanner (Varian Vnmrj 2.3A, Palo Alto, CA, USA) with 1 s temporal resolution, shown by the solid blue line in Fig. 2a. The pyr:lac ratio in the big disk was the same as in the original spectrum, and lactate amplitude in the small disk was multiplied by 6 in order to mimic elevated lactate level (inset in Fig. 2a). Zero-mean noise was added to both the real and imaginary channel to simulate SNR~25. A true image was generated for each echo at each time frame, and a raw projection line was calculated using Radon transform and then weighted by a factor that accounts for the longitudinal magnetization loss due to previous RF excitations, based on the following equation  $M_{xy}(k) = M_0(\cos \alpha)^{k-1} \sin \alpha$ , where  $\alpha$  is the flip angle and  $k$  is the index for the current excitation out of the entire scan. Finally, the proposed reconstruction method was applied to the simulated raw data. A phantom experiment of an HP urea C-13 syringe phantom was also conducted on the Varian scanner. Parameters were the same as in the simulation. A home-made H-1/C-13 dual-tuned surface coil was used with constant transmission power ( $FA \sim 10^\circ$ ) and  $FOV = 10$  cm.

For the simulation, the lactate image at the first time frame was selected and shown in Figs. 2c and 2d. Due to the high angular undersampling factor, the FBP algorithm results in severe streak artifacts (Fig. 2c). These streaks are significantly reduced by HYPR processing (Fig. 2d). In order to validate the temporal fidelity, the time course of pyruvate in the big disk and lactate in both disks are plotted in Fig. 2b. All measured signals (circles) show good agreement with the true time course (solid lines). In the HP C-13 experiment, the reconstructed urea HYPR image (Fig. 3b) showed less streak artifacts than the FBP (Fig. 3a). Fig. 3c shows the spectra of a  $5 \times 5$  ROI located in both syringes (1 and 2). The peak shift ( $\sim 24Hz$ ) is due to inhomogeneous shimming.

## RESULTS

For the simulation, the lactate image at the first time frame was selected and shown in Figs. 2c and 2d. Due to the high angular undersampling factor, the FBP algorithm results in severe streak artifacts (Fig. 2c). These streaks are significantly reduced by HYPR processing (Fig. 2d). In order to validate the temporal fidelity, the time course of pyruvate in the big disk and lactate in both disks are plotted in Fig. 2b. All measured signals (circles) show good agreement with the true time course (solid lines). In the HP C-13 experiment, the reconstructed urea HYPR image (Fig. 3b) showed less streak artifacts than the FBP (Fig. 3a). Fig. 3c shows the spectra of a  $5 \times 5$  ROI located in both syringes (1 and 2). The peak shift ( $\sim 24Hz$ ) is due to inhomogeneous shimming.

## DISCUSSION AND CONCLUSIONS

In this work, we presented a radial EPSI approach, which is combined with HYPR processing to image HP C-13 species in real-time with spatial undersampling. In the proposed approach, each time frame is spectrally fully-sampled by acquiring the same projection at many TEs, but is spatially undersampled. The spatial undersampling artifacts are further addressed by performing the HYPR algorithm along the time dimension to suppress streaks and increase image SNR, similar to the HYPR application in CE-MRA. This proposed acquisition can also be combined with other chemical shift separation methods, such as IDEAL (5), to further explore the sparsity of the C-13 spectrum and speed up the acquisition.

**ACKNOWLEDGEMENTS** We grateful acknowledge GE Healthcare for their assistance and NIH for funding support.

**REFERENCES** [1] Peters *et al.*, MRM 2007; 58:1001-1009 [2] Adalsteinsson *et al.*, MRM 1998; 39:889-898 [3] Mansfield *et al.*, MRM 1984; 1:370-386 [4] Mistretta *et al.*, MRM 2006; 55:30-40 [5] Reeder *et al.*, MRM 2005; 54:636-644

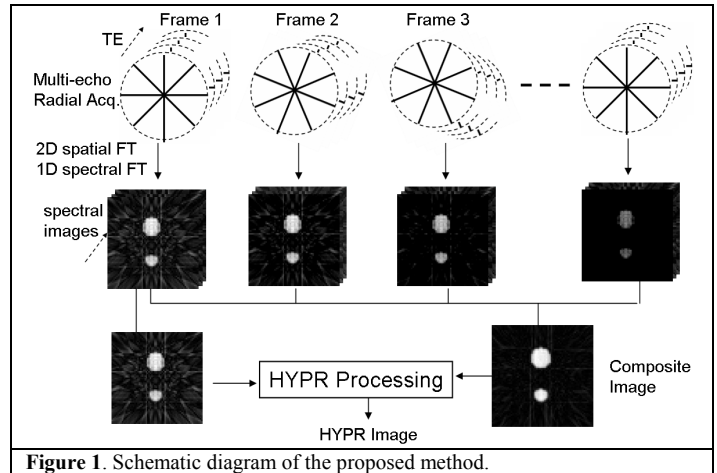


Figure 1. Schematic diagram of the proposed method.

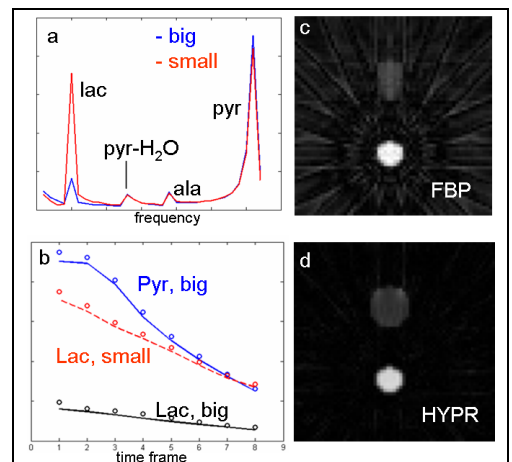


Figure 2. Simulation results. (a): Simulated spectra for the big and small disks at the first time frame. (b): Comparison between the true (solid lines) and the reconstructed (circles) temporal profiles. (c) and (d): Lactate images reconstructed by FBP and HYPR algorithms, respectively.

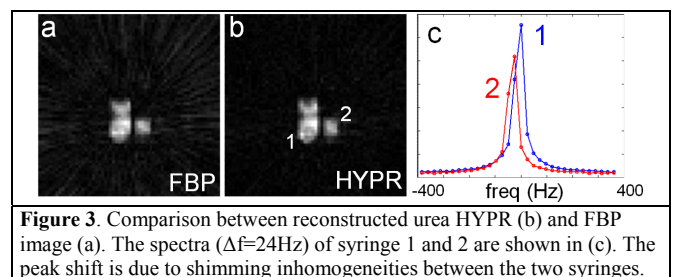


Figure 3. Comparison between reconstructed urea HYPR (b) and FBP image (a). The spectra ( $\Delta f=24Hz$ ) of syringe 1 and 2 are shown in (c). The peak shift is due to shimming inhomogeneities between the two syringes.